

First Keto-Functionalized Microporous Al-Based Metal–Organic Framework: [Al(OH)(O₂C-C₆H₄-CO-C₆H₄-CO₂)]

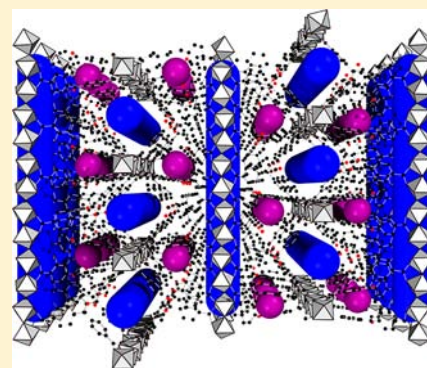
Helge Reinsch,[†] Martin Krüger,[†] Jerome Marrot,[‡] and Norbert Stock*[†]

[†]Institut für Anorganische Chemie, Christian-Albrechts-Universität zu Kiel, Max-Eyth-Straße 2, D-24118 Kiel, Germany

[‡]Institute Lavoisier (UMR CNRS 8180), Porous Solids Group, Université de Versailles Saint Quentin en Yvelines, 45, Avenue des Etats-Unis, 78035 Versailles, France

Supporting Information

ABSTRACT: Based on the V-shaped linker molecule 4,4'-benzophenonedicarboxylic acid, the new carbonyl-functionalized metal–organic framework (MOF) [Al(OH)(O₂C-C₆H₄-CO-C₆H₄-CO₂)], denoted as CAU-8, was discovered employing high-throughput methods. The compound is obtained from 4,4'-benzophenonedicarboxylic acid, Al₂(SO₄)₃·18H₂O in a mixture of *N,N*-dimethylformamide (DMF) and water under solvothermal conditions. The structure was determined from single-crystal X-ray diffraction data (*I*₄¹/*a*, *a* = *b* = 13.0625(5), *c* = 52.565(2) Å). The framework is based on infinite inorganic building units of *trans*-connected, corner-sharing AlO₆-polyhedra. Parallel Al–O-chains are arranged in layers perpendicular to [001]. Within a layer an interchain distance of ~1.1 nm is observed. The orientation of the Al–O-chains within neighboring layers is perpendicular to each other, along [100] and [010], respectively, and an ABCDA stacking of these layers is observed. The interconnection of these orthogonally oriented chains by the V-shaped dicarboxylate ions results in the formation of a three-dimensional framework structure containing one-dimensional channels with a diameter of about 8 Å. The pore walls are lined by the keto-groups. CAU-8 was thoroughly characterized by X-ray powder diffraction (XRPD), thermogravimetric measurements, IR- and Raman-spectroscopy, elemental analysis, and gas sorption experiments using N₂ and H₂ as adsorptives. CAU-8 is stable up to 350 °C in air and exhibits a moderate porosity with a specific surface area of *S*_{BET} = 600 m²/g and a micropore volume of 0.23 cm³/g. Moreover, a detailed topological analysis of the framework was carried out, and an approach for the topological analysis of MOFs based on infinite 1-periodic building units is proposed.



INTRODUCTION

Porous metal–organic frameworks (MOFs) are attracting considerable interest in academic as well as industrial research.^{1–3} The main reason for this is probably the opportunity to modulate their properties by crystal engineering. Once the synthesis of a new framework compound is established, the replacement of the building units by topologically identical ones during the synthesis allows in principle the tuning of the compound's properties.⁴ This was demonstrated for example for Al-MOFs based on linear dicarboxylate ions.^{5–9} The framework-topology of Al-MIL-53 (MIL stands for Matériaux de l'Institut Lavoisier) is based on the connection of linear chains of *trans*-connected corner-sharing AlO₆-polyhedra by dicarboxylate ions.⁵ Employing larger or smaller dicarboxylate ions, isorecticular compounds with altered pore size^{3,6,7} as well as chemically functionalized framework structures can be obtained.^{8,9} By alteration of the synthesis conditions, the formation of different inorganic nodes such as cyclic cationic clusters can be preferred, which lead to the formation of uninodal frameworks with cubic topology, denoted CAU-3 (CAU stands for Christian-Albrechts Universität).¹⁰ For this framework structure, the extension and the functionalization of the framework were only possible by employing high-throughput (HT) methods.¹¹ The change of the linker molecules can strongly affect the synthesis conditions

that allow the crystallization of the targeted compound, and HT-methods speed up the screening of large parameter spaces and thus ease the optimization of synthesis conditions.¹² We have focused our investigations on the synthesis of new aluminum-based MOFs, since these compounds have shown to be thermally and chemically very stable.¹³ Furthermore, Al³⁺ is nontoxic, and the inorganic reactants are inexpensive, which makes these MOFs interesting materials for industrial applications.³ Their stability allows the facile postsynthetic modification (PSM) of these compounds,^{14–16} which is a versatile method to generate functional groups in a MOF which are not accessible via conventional synthesis methods. Moreover a large variety of different functional groups can be readily introduced into Al-MOFs to “tune” their sorption properties.¹⁷

In this contribution, we report the solvothermal synthesis at the gram-scale of the new metal–organic framework [Al(OH)(O₂C-C₆H₄-CO-C₆H₄-CO₂)] denoted as CAU-8, based on 4,4'-benzophenonedicarboxylate. This compound was thoroughly characterized by single-crystal X-ray diffraction as well as X-ray powder diffraction (XRPD), thermogravimetric analysis, IR- and Raman-spectroscopy, elemental analysis, and gas

Received: September 7, 2012

Published: January 28, 2013

sorption measurements. Moreover its topology is described in detail.

EXPERIMENTAL SECTION

Chemicals. All chemicals are commercially available and were used as purchased, except for 4,4'-benzophenonedicarboxylic acid (H₂BPDC), which was ground prior to the synthesis.

Methods. HT-experiments were carried out in custom-made steel-multiclaves in Teflon-lined reaction vessels with a maximum volume of 2 mL.¹¹ The large-scale synthesis was carried out in a glass-reactor with screw-cap and a volume of 100 mL (DURAN GL 45). Single-crystal X-ray diffraction data was collected on a Bruker X8-APEX2 CCD area-detector diffractometer using Mo-K_{α1} radiation. X-ray powder diffraction data was collected on a STOE Stadi-P powder diffractometer in transmission geometry (Cu-K_{α1} radiation) using a linear position sensitive detector (PSD) system. SEM-micrographs were recorded on a Philips ESEM-XL 30 microscope. IR spectra were recorded on a Bruker ALPHA-FT-IR A220/D-01 spectrometer equipped with an ATR-unit. FT-Raman spectra were recorded on a Bruker IFS 66 FRA 106 spectrometer in the range of 0–3300 cm⁻¹ using a Nd:YAG-Laser (1064 nm). The thermogravimetric (TG) analyses were carried out using a NETSCH STA 409 CD analyzer. The samples were heated in Al₂O₃ crucibles at a rate of 4 K min⁻¹ under a flow of air (25 mL min⁻¹). The TG data were corrected for buoyancy and current effects. Gas sorption experiments were performed using a BEL JAPAN INC. Belsorp_{max} instrument. The programs used for the topological analysis were Systre¹⁸ and TOPOS.¹⁹

HT-Investigation. The solvothermal system Al³⁺/H₂BPDC/DMF/H₂O was investigated using different Al³⁺-sources. After discovery of CAU-8 (Figure 2), the synthesis parameters were systematically varied to optimize the purity and the crystallinity of the product. Different Al³⁺-sources were employed (Al(NO₃)₃·9H₂O, AlCl₃·6H₂O, and Al₂(SO₄)₃·18H₂O) and the absolute concentrations as well as the molar ratios of Al³⁺ and H₂BPDC were varied (30–200 g/L H₂BPDC; molar ratio Al³⁺:H₂BPDC between 2:1 and 1:1). The composition of the solvent mixture was altered as well (0–80 vol.% DMF). Moreover the influence of the pH was investigated using hydrochloric acid and sodium hydroxide as additives. The reaction time was varied between 12 and 36 h, and the temperature was varied between 120 and 145 °C. All samples were characterized by XRPD measurements.

Synthesis of Single Crystals of CAU-8. Single-crystals of CAU-8 suitable in size for the structure determination (Figure 1) were isolated

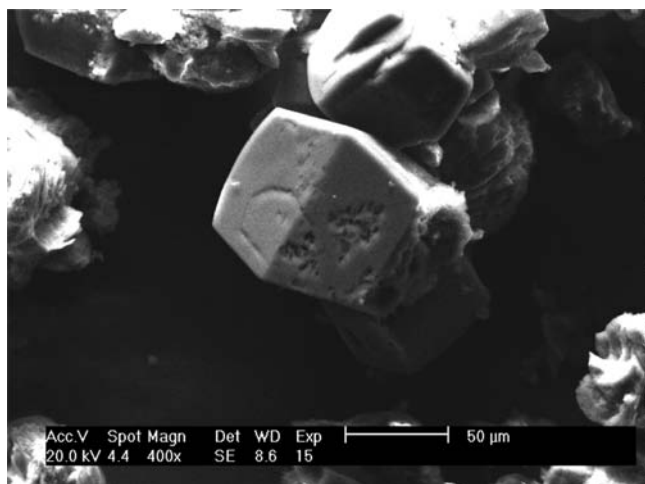


Figure 1. SEM-micrograph of a single crystal of CAU-8.

during the HT optimization experiments from a 2 mL-reactor. These were accompanied by a microcrystalline, unporous byproduct. In this experiment, 60 mg of H₂BPDC (0.22 mmol), 148 mg of Al₂(SO₄)₃·18H₂O

(0.22 mmol), 250 μL of DMF, and 250 μL of H₂O were heated in a HT-reactor up to 140 °C over 1 h, held at this temperature for 12 h, and cooled down to room temperature over 1 h.

Scale-Up Syntheses. Large amounts of phase-pure CAU-8 can be only obtained as microcrystalline powder after an additional activation step. For this synthesis, 2000 mg of H₂BPDC (7.4 mmol), 7.4 mL of a 0.5 M solution of Al₂(SO₄)₃·18H₂O (7.4 mmol Al³⁺), 0.6 mL of H₂O, and 12 mL of DMF (resulting volume ratio H₂O/DMF = 2:3) are heated in a HT-reactor up to 140 °C over 1 h, held at this temperature for 12 h, and cooled down to room temperature over 1 h. After filtration, a buff colored powder is obtained. This raw product contains recrystallized linker molecules, and therefore is treated with DMF (20 mL) at 85 °C overnight. After filtration, the now white solid is thoroughly washed with water and dried under ambient conditions. The yield is ~1.2 g (~40%). CHNS-analysis: N 1.6%, C 47.6%, H 3.4%. Calculated from the chemical formula [Al(OH)(O₂C-C₆H₄-CO-C₆H₄-CO₂)]·0.5DMF·3.7 H₂O: N 1.7%, C 47.7%, H 4.8%. The deviations from the theoretical value can be explained by the occlusion of small amounts of linker molecules inside the pores of the framework (see below). The absence of sulfur was proven by elemental analysis and EDX-analysis.

Structure Determination. A suitable single crystal was carefully selected and glued onto a glass fiber. The structure was solved using direct methods, developed by successive difference Fourier syntheses and refined by full-matrix least-squares on all F² data using SHELXTL. Diffuse electron density inside the framework due to occluded solvent molecules was corrected with the program SQUEEZE,²⁰ a part of the PLATON package of crystallographic software used to calculate the solvent or counterions disorder area and to remove its contribution to the overall intensity data. Results of the crystallographic work are summarized in Table 1. Crystallographic data for CAU-8 has been

Table 1. Crystal Data for CAU-8

empirical formula	C ₁₅ H ₆ AlO ₆
formula weight	312.20 g/mol
crystal system	tetragonal
space group	I4 ₁ /a (No. 88)
a = b, c [Å]	13.0625(5), 52.565(2)
V [Å ³]	8969.1(6)
Z	16
ρ(calc) [g/cm ³]	0.925
F (000)	2560
crystal size [mm]	0.02 × 0.06 × 0.08
temperature (K)	296
radiation [Å]	0.71073
θ min-max [deg]	1.5, 25.0
limiting indices	-15 > h > 15 -15 > k > 15 -62 > l > 62
reflections collected/unique	44877/3950
R(int)	0.112
observed data [I > 2σ(I)]	1901
number of reflections, parameters	3950, 205
R1	0.0791
wR2	0.2299
S	1.02
residual electron density [e/Å ³]	min. -0.20, max. 0.24

deposited with the Cambridge Crystallographic Data Centre as supplementary publication no. CCDC 899228. A copy of the data can be obtained, free of charge, on application to CCDC, 12 Union Road, Cambridge CB2 1EZ, U.K. (fax +44 1223 336033 or email deposit@ccdc.cam.ac.uk).

RESULTS AND DISCUSSION

HT Investigation. CAU-8 was discovered during the investigation of the system Al³⁺/H₂BPDC/DMF/H₂O under

solvothermal reaction conditions employing $\text{Al}(\text{NO}_3)_3 \cdot 9\text{H}_2\text{O}$ and $\text{Al}_2(\text{SO}_4)_3 \cdot 18\text{H}_2\text{O}$ as Al^{3+} -sources. In the first experiment that led to the discovery of CAU-8, the molar ratio $\text{Al}^{3+}/\text{H}_2\text{BPDC}$ was kept constant at 1:1, and the absolute concentration of the reactants as well as the ratio $\text{H}_2\text{O}/\text{DMF}$ was varied at a filling degree of 500 mL. The exact composition of the reaction mixtures can be found in the Supporting Information, Table S1. The experiment and the results which are based on XRPD measurements are visualized in Figure 2. Employing

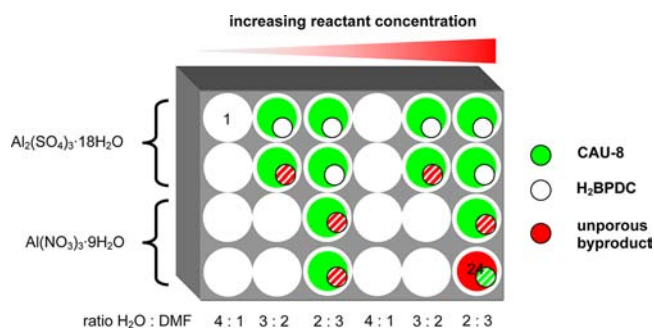


Figure 2. Schematic representation of the obtained products and the observed tendencies in the HT-experiment that led to the discovery of CAU-8. The results are based on the XRPD measurements.

both Al^{3+} -sources the formation of CAU-8 is observed. For $\text{Al}_2(\text{SO}_4)_3 \cdot 18\text{H}_2\text{O}$, the minimum amount of DMF necessary for the synthesis of CAU-8 is 200 μL while lower fractions of DMF result only in the recrystallization of H_2BPDC . Higher concentrations of the reactants induce the formation of a nonporous byproduct but lead also to better crystalline CAU-8 products. Using $\text{Al}(\text{NO}_3)_3 \cdot 9\text{H}_2\text{O}$ as Al^{3+} -source necessitates higher fractions of DMF (at least 300 μL) to induce the formation of CAU-8, and in all cases the formation of the byproduct is observed. At higher absolute concentrations the nonporous compound becomes the main product and CAU-8 is observed only in minor amounts. In general, less crystalline products are obtained when $\text{Al}(\text{NO}_3)_3 \cdot 9\text{H}_2\text{O}$ is employed as the Al^{3+} -source. Moreover, the recrystallized linker molecules were observed in all reaction vessels, but can be removed by washing in DMF. Further detailed HT-investigations (~150 reactions) optimizing the reactant concentrations, the temperature–time program, and the solvent ratio led to the optimized synthesis procedure, which could also be successfully up-scaled to larger reactors.

Crystal Structure of CAU-8. The crystal structure of CAU-8 was determined from single crystal X-ray diffraction data. The formation of single crystals of Al-based MOFs suitable for in-house acquisition of diffraction data is remarkable, and to the best of our knowledge it has only been reported once up to now.²¹ Most often Al-based MOFs are only obtained as microcrystalline products.^{22,23}

The asymmetric unit of CAU-8 contains two crystallographically independent Al^{3+} -ions bridged by one μ_2 -OH-group and one complete linker molecule (Figure 3, Supporting Information, Figure S1).

Some characteristic bond lengths are summarized in the Supporting Information, Table S2. The inorganic building unit of CAU-8 is an infinite linear chain of *trans*-connected, corner-sharing AlO_6 -polyhedra, and it is therefore identical to the building unit in the MIL-53 framework,⁵ but the arrangement of these units as well as the framework structure are substantially different. In MIL-53 all Al–O chains are parallel to each other, and each chain is connected to four neighboring

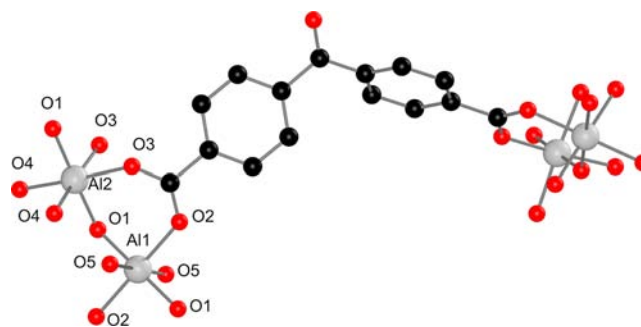


Figure 3. Extended asymmetric unit of CAU-8 displaying the coordination of the Al^{3+} -ions and the bridging nature of the ligand. Aluminum-atoms are shown as gray, oxygen-atoms as red, and carbon-atoms as black spheres. Hydrogen-atoms are omitted for clarity.

chains. Thus one-dimensional lozenge-shaped channels are formed. In contrast, in CAU-8 parallel chains of *trans*-connected, corner-sharing AlO_6 -polyhedra are arranged in layers of parallel chains with a distance of ~1.1 nm between each other. An ABCDA stacking of these layers is observed in which the chains in the layers A+C and B+D exhibit the same orientation (Figure 4, left). The orientation of the chains within neighboring layers is perpendicular to each other. The interconnection of two chains from adjacent layers is accomplished via four benzophenonedicarboxylate molecules as shown in Figure 4 (right), and thus a three-dimensional framework with one-dimensional channels is formed. The concave sides of the linker molecules surround small cavities ($\varnothing = 6.5 \text{ \AA}$), which possess very small windows with a diameter below 2 Å based on van der Waals radii. These windows are blocked by linker molecules of neighboring cages.

The convex sides of the linker molecules build up uniform, nonintersecting channels along [100] and [010] with a diameter of ~8 Å . The inner walls of the channels are lined with keto-groups (Figure 5).

The building units as well as the arrangement of the channels observed in CAU-8 are very similar to the ones recently reported for $[\text{In}(\text{OH})(\text{O}_2\text{C}-\text{C}_6\text{H}_4\text{OC}_6\text{H}_4-\text{CO}_2)]$.^{24,25} The structure of this compound is based on linear chains of *trans*-connected InO_6 -polyhedra which are interconnected by 4,4'-oxybisbenzoate ions. Thus the building units are very similar to the ones in CAU-8, but the connectivity is substantially different. While two chains are connected via four linker molecules at each crossing point in CAU-8, they are only connected by two linker molecules in the In-based MOF. Thus, $[\text{In}(\text{OH})(\text{O}_2\text{C}-\text{C}_6\text{H}_4\text{OC}_6\text{H}_4-\text{CO}_2)]$ exhibits a remarkable breathing effect, while CAU-8 possesses a rigid framework structure (Figure 7).

Thermal Stability and XRPD. According to the results of the TG measurement, the framework of CAU-8 decomposes at a temperature of 350 $^\circ\text{C}$ in air (Figure 6).

Up to a temperature of ~200 $^\circ\text{C}$, occluded solvent molecules (H_2O , DMF) are removed (mass loss: 17.5%), which is an endothermic reaction according to the DTA-curve. Between 200 and 350 $^\circ\text{C}$ a continuous mass loss is observed which can be attributed to the removal of small amounts of residual linker molecules from the pores. Above 350 $^\circ\text{C}$, the framework is decomposed in a strongly exothermic reaction. The mass loss above 350 $^\circ\text{C}$ (68.1%) is in very good agreement with the expected value (67.6%) based on the chemical formula $[\text{Al}(\text{OH})(\text{O}_2\text{C}-\text{C}_6\text{H}_4-\text{CO}-\text{C}_6\text{H}_4\text{CO}_2)]$. The XRPD-measurements further prove the thermal stability of the CAU-8

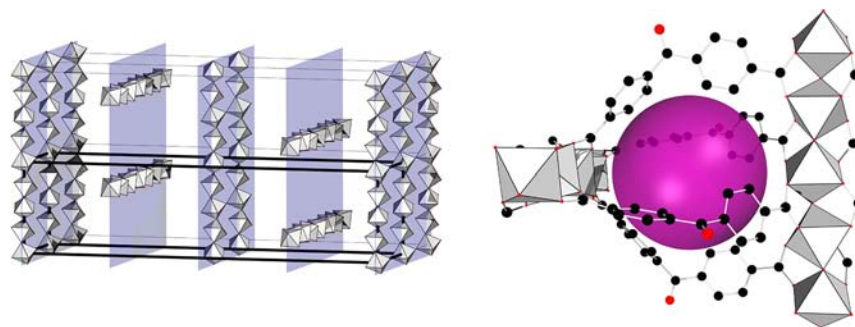


Figure 4. Left: ABCDA-stacking of the layers of AlO_6 -chains in a $2 \times 2 \times 1$ supercell as observed in the framework of CAU-8. The corresponding lattice planes are emphasized in blue. Right: Connection of two adjacent Al–O-chains via four benzophenonedicarboxylate molecules (both viewed along $[100]$). The cavity between the linker molecules is displayed as a purple sphere. The unit cell is shown in black, bold lines.

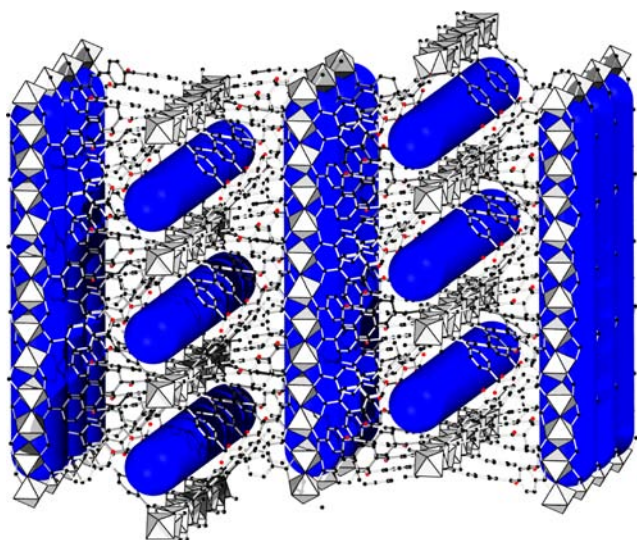


Figure 5. Representation of the framework structure of CAU-8. The keto-lined channels are represented as blue tubes. AlO_6 -polyhedra in gray, carbon atoms in black, oxygen atoms in red, hydrogen atoms were omitted for clarity.

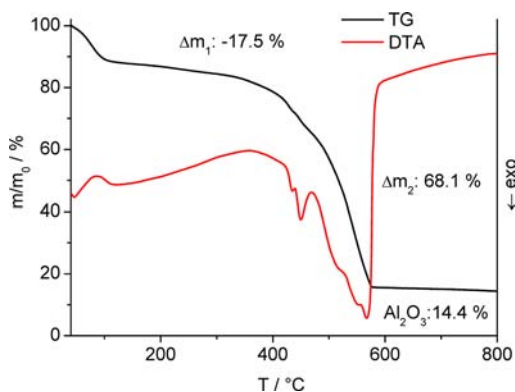


Figure 6. TG- and DTA-curves of CAU-8, measured with a heating rate of 4 K/min under air.

framework structure upon moderate thermal treatment. After activation under vacuum at 200 °C, no loss of crystallinity is observed, and the structure is fully retained (Figure 7). Furthermore, upon storage under ambient conditions, we did not observe any decomposition of the framework.

The rigidity of the framework is demonstrated since no shift of the Bragg peaks upon thermal treatment is observed.

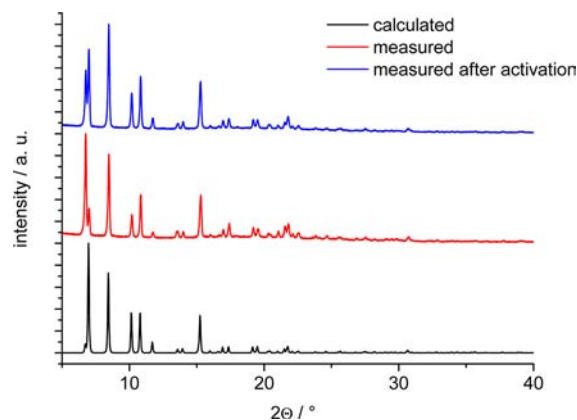


Figure 7. XRPD-data for CAU-8. Pattern calculated from single crystal data in black, experimental pattern of the MOF before activation in red, and after activation at 200 °C in vacuum in blue.

However, the relative intensities strongly vary. While the first peak at 6.7° has hardly any intensity according to single crystal data, it is the peak of highest intensity for the as synthesized CAU-8 and still shows high intensity in the activated product. We attribute this to the different amounts of guest molecules occluded inside the pores. These species are not taken into account in the single crystal structure, since the diffuse electron density of the disordered solvent and linker molecules was treated with the SQUEEZE routine during the structure determination. Upon removal of the solvent molecule, the relative intensities change substantially, but due to the small amount of occluded linker molecules they still deviate from the expected intensities deduced from the single crystal structure.

Vibrational Spectroscopy. The IR- and the Raman-spectra of CAU-8 are displayed in Figure 8. The most prominent band in both spectra is the asymmetric ν_{CO} -band of the carboxylate-groups at 1603 cm^{-1} . The absorption of the corresponding symmetric vibration can be observed at 1433 cm^{-1} . The ν_{CO} -band of the keto-group in the linker molecule is observed at 1667 cm^{-1} . Some residual linker molecules could not be removed by solvent treatment. The band at 1714 cm^{-1} can be attributed to the ν_{CO} -band of free carboxylic acid groups and is due to the inclusion of small amounts of linker molecules inside the channels. This result is consistent with the continuous mass loss between 200 and 350 °C observed in the TG-experiment (Figure 6).

The ν_{CH} -band of the aromatic ring is clearly observed in the Raman-spectrum at 3074 cm^{-1} . The δ_{CH} -band for

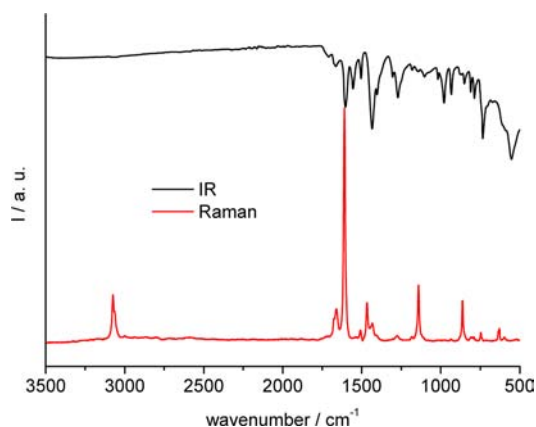


Figure 8. IR-spectrum (black line) and Raman-spectrum (red line) of CAU-8.

1,4-substituted benzene rings is found at 864 cm^{-1} . The ν_{CC} -band of the bond between the benzene core and the CO-group is observed at 1140 cm^{-1} .

Sorption Properties. Prior to the sorption measurement, the MOF was activated for 18 h at $200\text{ }^{\circ}\text{C}$ under vacuum (0.1 mbar). The nitrogen sorption experiment clearly yields a type-I-isotherm, proving the microporosity of CAU-8 (Figure 9).

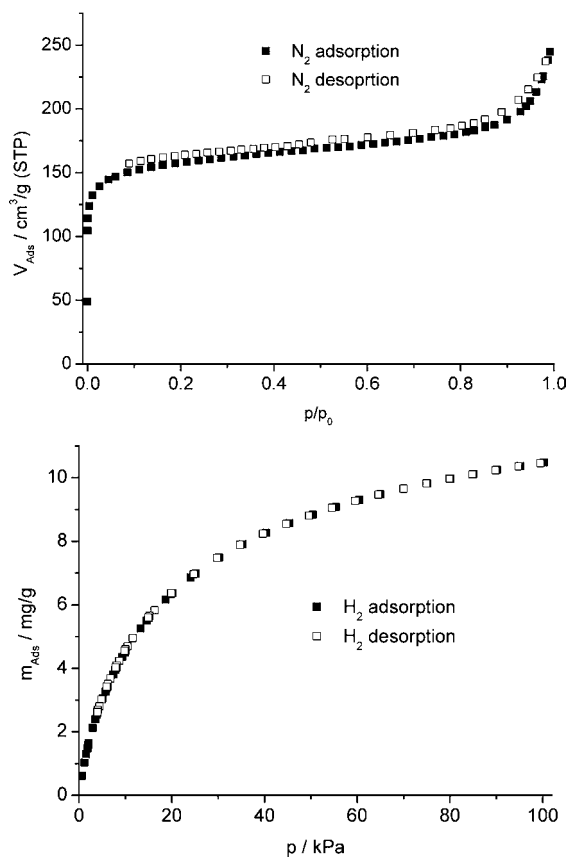


Figure 9. N_2 - and H_2 -sorption isotherms for CAU-8 measured at 77 K. Filled symbols represent the adsorption, empty symbols represent the desorption branch.

The specific surface area according to the Brunauer–Emmett–Teller (BET)-method is $S_{\text{BET}} = 600\text{ m}^2/\text{g}$, and the observed micropore volume is $V_{\text{MIC}} = 0.23\text{ cm}^3/\text{g}$, calculated from the

amount adsorbed at $p/p_0 = 0.5$. The maximum uptake of hydrogen at 77 K and 1 bar is 1.04 wt %.

Topological Analysis. The infinite aluminum-oxo-chain can be considered in different ways for the topological analysis. It was recently proposed,²⁶ to object to such an infinite building unit as a ladder-like fragment of the network. This expands the one-periodic building unit into a two-dimensional fragment. However, in nearly all cases for MOFs based on finite inorganic building units, the zero-periodic character of the building blocks is retained by merging the points of extension into a “zero-dimensional” point for the topological classification. Therefore, we consider a different approach for the handling of the one-periodic building unit in CAU-8, which does not convert the infinite chain into a ladder-like fragment, but into a zigzag-line for the topological analysis (Figure 10). In this approach two points of extension are merged into one.

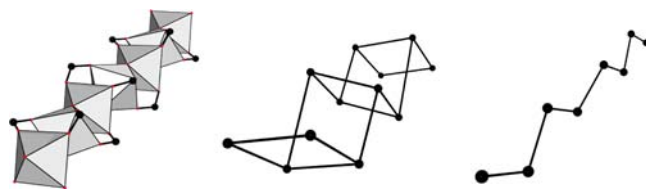


Figure 10. Part of the infinite chain as observed in CAU-8 (left), the ladder like model (middle), and the zigzag-line (right) used for the topological analysis in this contribution.

For the topological analysis the embedding of highest symmetry was calculated using the program Systre.¹⁸ Subsequently this embedding was further analyzed with TOPOS.¹⁹ According to this procedure, the underlying net of CAU-8 has been reported, but no three-letter code has been assigned up to now. The net is an uninodal, four-connected 4/5/t1 net with the point symbol $5^4.8^2$ (Figure 11). The vertex symbol of this net is

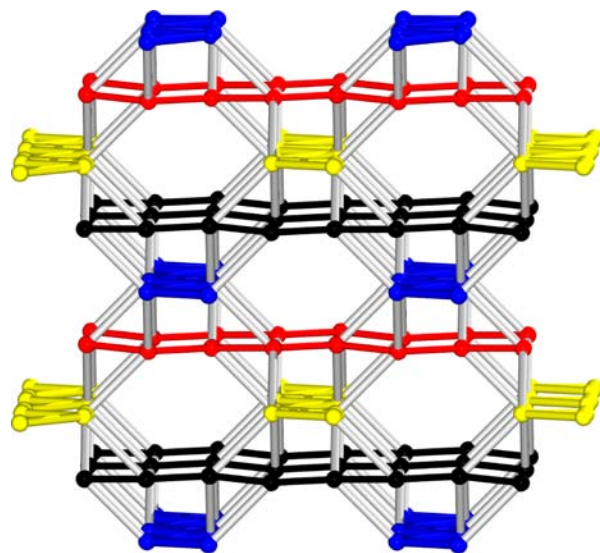


Figure 11. Representation of the underlying net of CAU-8 as seen along the b -axis. The fragments which represent the Al-oxo-chains are emphasized in blue, black, yellow, and red, corresponding to the respective layer. The bonds between the colored chains (gray) represent the V-shaped organic moieties.

$5.5_2.5.8.5.8$. The notation 4/5/t1 was introduced by Fischer, who reported on tetragonal homogeneous sphere packings.²⁷

This representation in the form $k/l/tm$ describes that every vertex has k nearest neighbors and that the shortest circuit is an l -ring. The t represents the crystal system, in this case tetragonal, while m is a number.

This net is a very accurate representation of the CAU-8-framework. The character of the Al–O chains can be clearly identified in the topology (emphasized in blue, black, yellow, and red in Figure 10) as well as the arrangement in an ABCD-fashion. Thus, the one-periodic character of the inorganic units as well as the structural features of the MOF is retained. To set this result in a broader context, we have applied this procedure to various other MOFs, which are based on infinite, one-periodic building units. Thus this analysis was carried out for the frameworks of MIL-53,⁵ MIL-68,²⁸ CAU-4,²⁹ CAU-6,³⁰ and CAU-10.¹⁷ In all cases we observed a very accurate representation of the underlying net for the selected frameworks by merging adjacent points of extension whenever appropriate (Supporting Information, Figures S2–S11, Table S3).

CONCLUSIONS

CAU-8 is a rare example of a keto-functionalized MOF and was readily synthesized from commercially available chemicals. It extends the number of framework structures of MOFs based on linear chains of *trans*-connected M(III)O₆-polyhedra of which the most important members are the ones of the MIL-53-family. The keto-group should be chemically accessible, and thus postsynthetic modification reactions should be feasible. First studies have been carried out by us, but the reactivity seems to be inferior compared to MOFs containing aldehyde groups. The proposed topological approach toward the handling of infinite one-periodic building units shows promising results and could turn out as a versatile method for the classification of such materials.

ASSOCIATED CONTENT

Supporting Information

Exact composition of the reaction mixtures in the high-throughput experiment; the asymmetric unit and selected bond lengths; topological analysis of MOFs based on infinite one-periodic building units. This material is available free of charge via the Internet at <http://pubs.acs.org>.

AUTHOR INFORMATION

Corresponding Author

*E-mail: stock@ac.uni-kiel.de.

Notes

The authors declare no competing financial interest.

ACKNOWLEDGMENTS

This work has been supported by the DFG (SPP 1362). The research leading to these results has received funding from the European Community's Seventh Framework Programme (FP7/2007–2013) under grant agreement no 228862.

REFERENCES

- (1) Stock, N.; Biswas, S. *Chem. Rev.* **2012**, *112*, 933–969.
- (2) Janiak, C.; Vieth, J. K. *New J. Chem.* **2010**, *34*, 2366–2388.
- (3) Gaab, M.; Trukhan, N.; Maurer, S.; Gummaraju, R.; Müller, U. *Microporous Mesoporous Mater.* **2012**, *157*, 131–136.
- (4) O'Keeffe, M. *Chem. Soc. Rev.* **2009**, *38*, 1215–1217.
- (5) Loiseau, T.; Serre, C.; Huguenard, C.; Fink, G.; Taulelle, F.; Henry, M.; Bataille, T.; Férey, G. *Chem.—Eur. J.* **2004**, *10*, 1373–1382.

- (6) Senkovska, I.; Hoffmann, F.; Fröba, M.; Getzschmann, J.; Böhlmann, W.; Kaskel, S. *Microporous Mesoporous Mater.* **2009**, *122*, 93–98.
- (7) Biswas, S.; Ahnfeldt, T.; Stock, N. *Inorg. Chem.* **2011**, *50*, 9518–9526.
- (8) Comotti, A.; Bracco, S.; Sozzani, P.; Horike, S.; Matsuda, R.; Chen, J.; Takata, M.; Kubota, Y.; Kitagawa, S. *J. Am. Chem. Soc.* **2008**, *130*, 13664–13672.
- (9) Reimer, N.; Gil, B.; Marszalek, B.; Stock, N. *CrystEngComm* **2012**, *14*, 4119–4125.
- (10) Reinsch, H.; Feyand, M.; Ahnfeldt, T.; Stock, N. *Dalton Trans.* **2012**, *41*, 4164–4171.
- (11) Stock, N. *Microporous Mesoporous Mater.* **2010**, *129*, 287–295.
- (12) Sonnauer, A.; Hoffmann, F.; Fröba, M.; Kienle, L.; Duppel, V.; Thommes, M.; Serre, C.; Férey, G.; Stock, N. *Angew. Chem., Int. Ed.* **2009**, *48*, 3791–3794.
- (13) Cychosz, K. A.; Matzger, A. J. *Langmuir* **2010**, *26*, 17198–17202.
- (14) Ahnfeldt, T.; Gunzelmann, D.; Loiseau, T.; Hirsemann, D.; Senker, J.; Férey, G.; Stock, N. *Inorg. Chem.* **2009**, *48*, 3057–3064.
- (15) Goesten, M. G.; Stavitski, E.; Juan-Alcaniz, J.; Ramos-Fernandez, E. V.; Sai Sankar Gupta, K. B.; van Bekkum, H.; Gascon, J.; Kapteijn, F. *J. Catal.* **2011**, *281*, 177–187.
- (16) Ahnfeldt, T.; Gunzelmann, D.; Wack, J.; Senker, J.; Stock, N. *CrystEngComm* **2012**, *14*, 4126–4136.
- (17) Reinsch, H.; Van der Veen, M. A.; Gil, B.; Marszalek, B.; Verbiest, T.; De Vos, D.; Stock, N. *Chem. Mater.* **2013**, *25*, 17–26.
- (18) Delgado-Friedrichs, O.; O'Keeffe, M. *Acta Crystallogr., Sect. A* **2003**, *59*, 351–360.
- (19) Blatov, V. A. *Crystallogr. Rev.* **2004**, *10*, 249–318.
- (20) van der Sluis, P.; Spek, A. L. *Acta Crystallogr., Sect. A* **1990**, *46*, 194.
- (21) Loiseau, T.; Lecroq, L.; Volkringer, C.; Marrot, J.; Férey, G.; Haouas, M.; Taulelle, F.; Bourrelly, S.; Llewellyn, P. L.; Latroche, M. J. *Am. Chem. Soc.* **2006**, *128*, 10223–10230.
- (22) Ahnfeldt, T.; Guillou, N.; Gunzelmann, D.; Margiolaki, I.; Loiseau, T.; Férey, G.; Senker, J.; Stock, N. *Angew. Chem., Int. Ed.* **2009**, *28*, 5163–5166.
- (23) Fateeva, A.; Chater, P. A.; Ireland, C. P.; Tahir, A. A.; Khimiyak, Y. Z.; Wiper, P. V.; Darwent, J. R.; Rosseinsky, M. J. *Angew. Chem., Int. Ed.* **2012**, *51*, 7440–7444.
- (24) Jin, Z.; Zhao, H.-Y.; Zhao, X.-J.; Fang, Q.-R.; Long, J. R.; Zhu, G.-S. *Chem. Commun.* **2010**, *46*, 8612–8614.
- (25) Tan, Y.-X.; Wang, F.; Kang, Y.; Zhang, J. *Chem. Commun.* **2011**, *47*, 770–772.
- (26) O'Keeffe, M.; Yaghi, O. M. *Chem. Rev.* **2012**, *112*, 675–702.
- (27) Fischer, W. Z. *Kristallogr.* **1993**, *205*, 9–26.
- (28) Volkringer, C.; Meddouri, M.; Loiseau, T.; Guillou, N.; Marrot, J.; Férey, G.; Haouas, M.; Taulelle, F.; Audebrand, N.; Latroche, M. *Inorg. Chem.* **2008**, *47*, 11892–11901.
- (29) Reinsch, H.; Krüger, M.; Wack, J.; Senker, J.; Salles, F.; Maurin, G.; Stock, N. *Microporous Mesoporous Mater.* **2012**, *157*, 50–55.
- (30) Reinsch, H.; Marszalek, B.; Wack, J.; Senker, J.; Gil, B.; Stock, N. *Chem. Commun.* **2012**, *48*, 9486–9488.